ELSEVIER

Chemical Engineering Journal 137 (2008) 376–385

Chemical Engineering Journal

www.elsevier.com/locate/cej

Gamma ray tomography—An experimental analysis of fractional gas hold-up in bubble columns

Ashutosh K. Patel, Bhaskar N. Thorat *

Chemical Engineering Department, Institute of Chemical Technology (ICT), N.M. Parekh Road, Matunga (E), Mumbai, Maharashtra 400019, India

Received 25 July 2006; received in revised form 27 April 2007; accepted 2 May 2007

Abstract

Gas hold-up is one of the most important hydrodynamic parameters involved in the design, development, scale-up and troubleshooting of multiphase systems. Gamma ray tomography (GRT) is an extensively used non-destructive and non-invasive technique for the measurement of the gas hold-up profiles in multiphase system such as bubble columns and stirred vessels. The tomographic measurements can be subsequently used for the qualitative as well as quantitative estimation of the performance of multiphase system under given set of operating conditions. The non-destructive technique of grid scanning which forms the basis of GRT was used to analyze the performance of the laboratory scale bubble column as well as industrial scale sectionalized bubble column. The later had a total height of 8.5 m divided into 10 equal sections. The hydrodynamic performance obtained in the form of chordal gas hold-up was shown to be highly influenced as a result of the sparger design altercations. The non-performance of spargers due to the hole blockage was studied in a bubble column of 0.2 m diameter by analyzing the reconstructed gas hold-up profile at two different axial locations. An industrial sectionalized bubble column was also studied to obtain the desired information on the change in gas hold-up in the axial direction as a result of increased $\bar{\varepsilon}_G$ due to intrinsic reaction kinetics giving rise to the formation of additional gas at every stage.

Keywords: Algebraic reconstruction technique; Pressure drop; Sparger design; Chordal hold-up; Grid scanning

1. Introduction

The extensive understanding of multiphase system hydrodynamics is needed for the design and development of an optimized and trouble free operation. Design and scale-up of bubble columns, slurry bubble columns, three phase fluidized beds and other multiphase systems are still predominantly based on empirical correlations, validated over a limited range of operating conditions and physical properties. Application of more fundamental fluid dynamic models awaits the experimental validation. The measurement of fluid dynamic quantities such as phase velocities, phase hold-ups, bubble size, etc. are of great interest for extending the range of validity of current correlations and for verification of fundamental hydrodynamic models based on computational fluid dynamics (CFD). The measurement of multiphase system parameters are equally important for interpreting, understanding and predicting the overall performance as shown in Fig. 1. Modern reactor engineering, utilizes series of tools and techniques of instrumentation and signal processing methods, which lead to a confidence building exercise amongst the engineers and scientists. These tools include a variety of tomographic imaging methods for the determination of the spatial and temporal distribution of various process variables and diagnostic determination of process problems. The tools and techniques that cover the aforementioned types of measurements and predictions fall under the general name of "Process Tomography". Applications of process tomography in the laboratory and industry have become necessity rather than a mere curiosity. This is evidenced from the large number of studies reported in the literature [1–5]. The assessment of the performance of a multiphase system can now be done using area measurements as opposed to the point measurements (i.e., sensors) which were conventionally used in earlier days. The incorporation of tomographic measurements in process models will lead to a new generation of design procedures for reactors.

* Corresponding author. Tel.: +91 22 24145616x289; fax: +91 22 24145614.
E-mail addresses: bnt@udct.org, bnthorat@udct.org (B.N. Thorat).

1385-8947/$ – see front matter © 2007 Elsevier B.V. All rights reserved.
doi:10.1016/j.cej.2007.05.014

Nomenclature

A	attenuation
A_{RS}	arithmetic average plate free area of sectionalizing plates and sparger
a	element of system matrix/weighted matrix
d	distance of projection from the center of the column (m)
D	diameter of column (m)
D_{AS}	arithmetic average hole diameter of sectionalizing plates and sparger (m)
H_D	dispersed liquid height (m)
H_L	clear liquid height (m)
I	intensities of the emerging beam of gamma rays (counts/s)
I_0	intensities of the incident beam of gamma rays (counts/s)
l_{ij}	the length of jth projection in ith pixel (m)
M	total number of projections
n	number of plate including sparger
N	total number of pixels
p	projection
$\bar{p}$	projection estimated
S	system matrix/weighted matrix
t	path length/thickness of absorbing medium (m)
U_L	volumetric liquid flow rate (m^3/h)
V_D	dispersed volume of column (m^3)
V_G	superficial gas velocity (m/s)
z_j	the number of pixels through which jth projection passes

Greek letters

ε	fractional gas hold-up
ε_{chord}	chordal hold-up
$\bar{\varepsilon}$	average gas hold-up
θ	source angle (°)
τ	residence time (h)
μ	linear attenuation coefficient (m^{-1})

Subscripts

chodl	chordal gas hold-up
G	gas
i	number of pixel
j	number of projection
k	number of iteration
L	liquid
TP	two phases
w	wall

Process tomography has been a useful tool for broad range of chemical engineering processes involving multiphase systems such as bubble column, packed bed, fluidized bed, trickle bed reactor, distillation column, pneumatic transport, liquid mixing, cyclonic separation, pressure filtration, liquid pipe-flow, polymerization, emergency de-pressurization, paste extrusion and so on. Tomographic technique involves the acquisition of measurement signals obtained from the sensors located on the periphery of process vessels. A wide range of computer tomographic techniques are available depending on the form of energy used in reference with the measuring phase characteristics, such as ultrasound (ultrasonic tomography), electrical (electrical resistance tomography and electrical capacitance tomography), nucleonic (X-ray or γ-ray tomography), optical (optical tomography) and so on. Process tomography gives information on cross-sectional profiles of the phases in a process equipment. There are number of good reviews of these measurement techniques that discuss their capabilities and constrains [6–11].

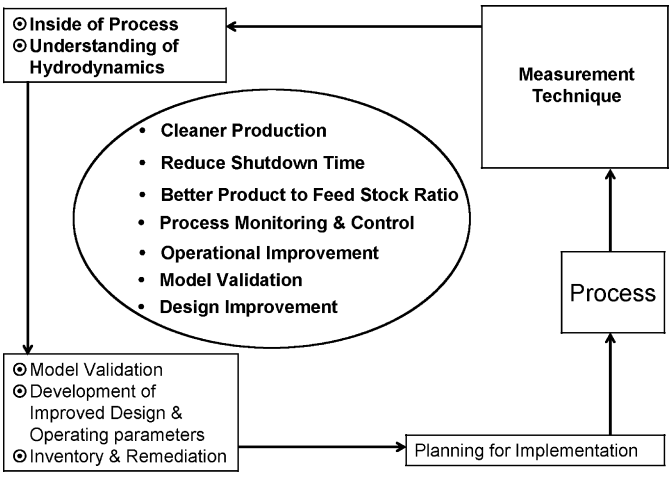

Fig. 1. Schematic of importance of measurement techniques in chemical industries.

Bubble columns are extensively used in chemical, biochemical and metallurgical industry because of their simple construction and ease of operation. Important applications include oxidation, hydrogenation, halogenation, hydrohalogenation, ammonolysis, hydroformylation, carbonylation, carboxylation, Fischer–Tropsch reaction, ozonolysis, alkylation, fermentation, waste water treatment and so on. It is well accepted that gas sparger design and its performance can have a significant effect on both the local and overall gas hold-up in bubble column reactors. The use of computational fluid dynamics to provide a priori predictions of performance for variety of commercial-scale spargers is not possible using existing knowledge. This is mainly due to the existence of a large number of sparger holes that are typically present in a commercial-scale gas sparger, and the difficulties associated with modeling high velocity and multiple interacting gas jets into gas–liquid dispersion [12,13]. The knowledge of radial as well as axial gas hold-up distribution is vital in understanding the fluid dynamics to a greater extent as it gives rise to pressure variation resulting in a characteristic liquid circulation in a bubble column. This intern governs the rate of the mixing and the transport process occurring in the reactor. Gas hold-up information also facilitates the determination of the flow regime (such as homogeneous, transition and heterogeneous regime) of operation for a given set of operating conditions. It is well reported that the γ-ray tomography is capable of measuring phase distribution in a small to large size (widely configured) multiphase system over a broad range of operating parameters.

In the present work, a laboratory and an industrial scale bubble column was studied using gamma ray tomography. The purpose was to obtain the gas hold-up profile both, axially as well as radially. The data intern could be used for the validation of the mathematical model, which can be then used as an less expensive tool for newer reactor design or retrofitting of the existing bubble column. The scanned data was subsequently used for qualitative as well as quantitative estimation of the system performance under current set of operating conditions. The conventionally used bubble column and the modified form of bubble column (sectionalized bubble column) were analyzed from the point of view of local gas hold-up distribution. A perforated plate sparger having large number of holes was deliberately blocked partially to study the effect of sparger blockage on the gas hold-up distribution.

2. Gamma ray tomography: underlying principle

Gamma rays emitted during the radioactive decay process fly off and penetrate through the multiphase system area and can be detected by scintillation detectors placed on the opposite side of the source. Detector catches the coincidentally emitted γ-rays and the attenuation taken place inside the volume between the source and the detector. The attenuation (A) is a function of the attenuation coefficient, μ (which intern depends on the energy possessed by gamma photons and phase density) and the thickness of the absorber. It can be expressed on the basis of Beer's Lambart law as follow:

$$A = -\ln\left[\frac{I}{I_0}\right] = \int \mu \, \mathrm{d}t \tag{1}$$

where I_0 and I are the intensities of the incident and emerging beams, respectively; μ the linear attenuation coefficient; t the thickness of the absorbing medium; and A is the attenuation. From Eq. (1), it can be seen that the attenuation and the attenuation coefficient are linearly related. The attenuation of the γ-rays through a bubble column filled with gas, liquid and gas–liquid medium can be given by the following expressions, respectively:

$$\ln\left[\frac{I_\mathrm{G}}{I_0}\right] = -(\mu_\mathrm{G} t_\mathrm{G} + \mu_\mathrm{w} 2t_\mathrm{w}) \tag{2}$$

$$\ln\left[\frac{I_\mathrm{L}}{I_0}\right] = -(\mu_\mathrm{L} t_\mathrm{L} + \mu_\mathrm{w} 2t_\mathrm{w}) \tag{3}$$

$$\ln\left[\frac{I_\mathrm{TP}}{I_0}\right] = -(\mu_\mathrm{G} t'_\mathrm{G} + \mu_\mathrm{L} t'_\mathrm{L} + \mu_\mathrm{w} 2t_\mathrm{w}) \tag{4}$$

Chordal gas hold-up of each measured projection, which is a linear integration of the local hold-up over projection path can be estimated using the following expression based on Eqs. (2)–(4):

$$\varepsilon_\mathrm{Chodl} = \frac{\ln(I_\mathrm{TP}/I_\mathrm{L})}{\ln(I_\mathrm{G}/I_\mathrm{L})} \tag{5}$$

The spatial distribution of gas hold-up can be reconstructed using a suitable reconstruction algorithm, provided the spatial variation of the chordal gas hold-up across the interested system area at several radial and angular locations is known.

3. Algebraic reconstruction technique (ART)

The iterative algorithm such as ART can be used for the image reconstruction because of its good flexibility for various beam configurations. Iterative method used for the estimation of attenuation distribution, can be expressed using the following equation [14]:

$$p_j = \sum_{i=1}^{N} a_{i,j}\mu_i \tag{6}$$

where p_j is the total attenuation measured at jth projection; N the total number of pixels; and μ_i is the attenuation coefficient value of ith pixel. $a_{i,j}$ is a parameter of system matrix or weighted matrix given by, $S = [a_{i,j}] \in \Re^{MN}$, which enables the iterative reconstruction method to recover resolution that was lost in the projections due to the measurement uncertainties. Fundamentally, iterative algorithm finds the solution of Eq. (6) by successive iterations.

The ART algorithm has been reported to work well with a limited number of path integral concentrations and projection angles. The ART algorithm is simply based on corrective technique. Each projected density is thrown back across the reconstruction space in which the densities are iteratively modified to bring each reconstructed projection into agreement with the measured projection. The estimated projection is subtracted from the measured projection and further used to estimate the accurate attenuation distribution by incorporating difference between the two in the current estimate. Conventionally, the iterative process is expressed as [14]:

$$\mu_i^{(k+1)} = \mu_i^{(k)} + \frac{p_j - \bar{p}_j}{N} \tag{7}$$

In the present study, the conventional ART expression given by Eq. (7) was modified to improve the reconstruction image quality and also to improve the flexibility to handle number of projections in different beam configuration and it is given by following equation:

$$\mu_i^{(k+1)} = \mu_i^{(k)} + \frac{p_j - \bar{p}_j}{\sum_{i=1}^{N} a_{ij}} a_{ij} \tag{8}$$

The iteration process is initiated by arbitrarily creating the first estimate. For example, a uniform image can be initialized to zero or by using non-uniform image initialization as described by Patel et al. [15]. In the present study, modified back-projection method has been used for image initialization and it can be expressed as

$$\mu_i = \frac{1}{M}\sum_{j=1}^{M} \frac{p_{ij}}{z_j} a_{ij} \tag{9}$$

where z_j is the number of pixels through which jth projection passes and a_{ij} is the system matrix element. Iterative process will continue till second term on right hand side in Eq. (8) becomes smaller than the threshold limit.

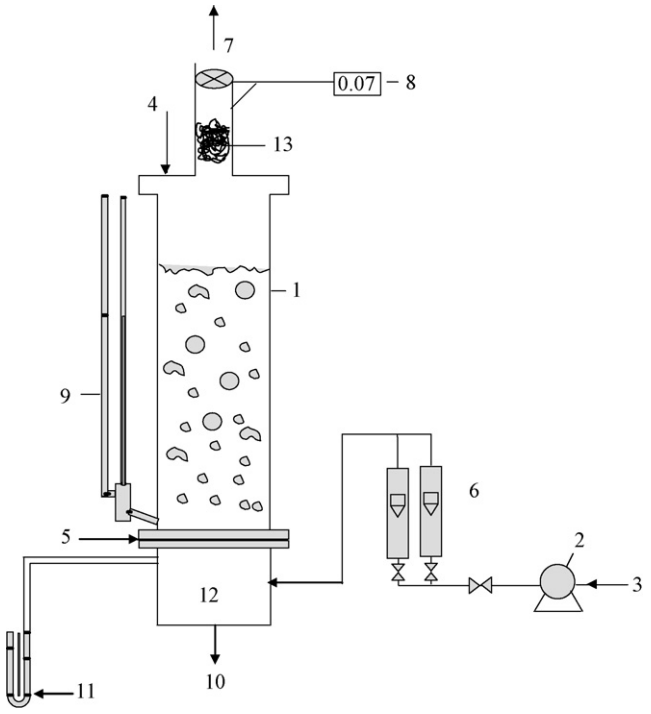

Fig. 2. Experimental set-up. 1, bubble column; 2, air compressor; 3, air inlet; 4, liquid inlet; 5, pipe sparger; 6, rotameter; 7, turbine anemometer; 8, anemometer display; 9, clear liquid tube; 10, liquid drain; 11, U-tube manometer; 12, gas chamber; 13, wire mesh.

4. Experimental

4.1. Experimental set-up

The schematic diagram of experimental apparatus is as shown in Fig. 2. Experiments were carried out in a cylindrical bubble column of 0.2 m i.d. and 1.2 m height. Perforated plate sparger (see Table 1) was placed between the column and the distribution chamber, which had a drain at the bottom and a gas inlet at the side. The column, gas distribution chamber and perforated plate spargers were made up of transparent acrylic material to enable visual observation of the gas hold-up and other column performances. Air and water were used as the gas and liquid phase, respectively. Experiments were carried out in a semi-batch manner. Perforated plates were employed having percent free area in the range of 0.42–6% and hole diameters of 0.001 and 0.003 m. The superficial gas velocity (V_G) was measured using anemometer placed at the top (exit) of the column. Polypropylene mesh was provided just before the anemometer to avoid the water entrainment by the gas. The effect of sparger opening was studied systematically by deliberately clogging the perforated plate (0.42% free area and 1 mm hole size) to the extent of 75%, 50% and 0% (fully open). GRT measurements were also carried out on an industrial scale sectionalizing bubble column reactor of 0.3 m diameter and 0.5 m^3 volume. The column was divided in 10 equal sections and each section separated by a perforated plate having % free area of 0.4. Sectionalizing column was operated in a continuous manner with respect to both gas and liquid phase. The column was operated counter-current wise with liquid coming from top and gas sparging from the bottom. Downcomer of 0.05 m diameter having sufficient length was provided at each sectionalizing plate for the exchange of only liquid between two consecutive sections.

Table 1
Geometric details of the spargers

Sparger	S1	S2	S3	S4
% free area	0.136	0.42	1	0.42
Hole dia. (mm)	1	1	1	3
Pitch (mm)	26	16	9.5	43
No. of holes	55	168	400	19

The experimental set-up for the measurement of gas hold-up by GRT technique is as shown in Fig. 3. It consists of ^{137}Cs gamma ray source (strength: 1 mCi and disc source of 0.02 m diameter), sodium iodide (NaI) with thallium (Tl) activated scintillation detectors (BICRON), photo multiplier tube, a preamplifier, a multi-channel (eight channels) analyzer, data acquisition system and related hardware and software. Source was collimated, having a slit of 0.03 m long and 0.003 m thickness. Circular collimators of 0.06 m diameter, having slit dimensions of 0.025 m long and 0.003 m thick were used.

4.2. Experimental methodology

Experiments for the measurement of fractional gas hold-up were carried out starting with the highest V_G and H_L/D. The clear liquid height was measured using side limb. The airflow rate was measured using anemometer. About five to six readings were taken for different superficial gas velocities, in the range of 0.01–0.3 m/s. The average fractional gas hold-up ($\bar{\varepsilon}_G$) was then calculated as $(H_D - H_L)/H_D$. The same procedure was repeated for other H_L/D ratios, running down from 3 to 1.

In gamma ray tomography of 0.2 m i.d. bubble column, fan beam scanning was employed and tomographic measurements were carried out at different axial ($H_L/D = 0.785$ and 2.75) locations and radial positions. At each axial location, source was placed at nine different positions at an interval of 40° and nine detectors were placed on opposite side equiangularly at 6° for each source position. GRT of industrial scale sectionalized bubble column reactor was carried out at four different sections (6th, 7th, 8th, and 9th section from bottom to top) to obtain gas hold-up profile. In each section the measurements were carried out at the location 0.37 m above the sectionalizing plate. Fan beam configuration was employed for the measurements.

Several trial runs were conducted with different combinations of dwell time and number of events. A dwell time of roughly 10 s was found to satisfactorily capture the steady state dynamic behavior of the flow pattern prevailing in the bubble column. An increase in dwell time would result in more precise representation of flow patterns. The two-phase counts were checked with the background counts. Based on these preliminary results, the number of events and dwell time were fixed at 50 and 10 s, respectively. This gave reproducibility of measurements within ±5%. The total acquisition time for each source position measurement was 500 s. The advantage of faster data acquisition would obviously depend on the combination of dwell time and

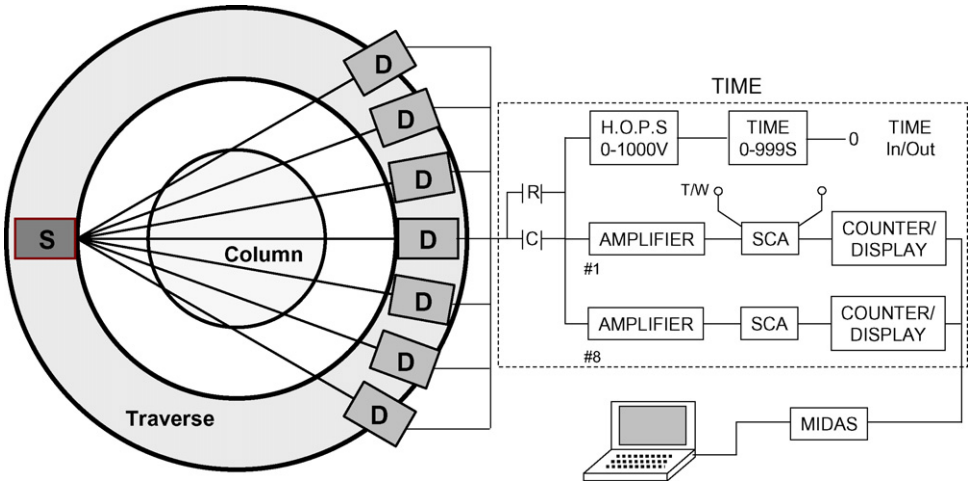

Fig. 3. Gamma ray scanning system. S, 1 mCi ^{137}Cs gamma source and D, 1 in. NaI(Tl) detector.

number of events. The restriction on the requirement of minimum dwell time would necessitate reduction in the number of events, reducing the total scan time. A move towards faster acquisition would therefore come at a cost of decreased overall accuracy. Every measurement gave the value of chordal gas hold-up. In the case of sectionalizing bubble column, the number of events and dwell time were fixed at 50 and 15 s, respectively. Local gas hold-up were calculated using the chordal gas hold-up values by applying the ART method as discussed earlier in Section 3.

5. Result and discussions

The present paper is divided in two parts. The first part covers the analysis of bubble column performance under various operating conditions. Thus, the effect of superficial gas velocity, free area and the sparger geometry on the fractional gas hold-up was studied. This is followed by the case study of industrial sectionalized bubble column reactor where the operating parameters were fixed and the analysis was done for the limited set of given parameters.

5.1. Efficacy of GRT to get insight of bubble column

5.1.1. Effect of superficial gas velocity

As anticipated, with an increase in superficial gas velocity, the average gas hold-up increases as shown in Fig. 4. For sparger hole diameter of 0.001 m, the fractional gas hold-up increases with an increase in free area and this is evident for the case of spargers, S1, S2 and S3. Thorat et al. [16] have reported similar observations for the bubble column of 0.385 m diameter. It can be seen from this figure that the average fractional gas hold-up obtained using bed expansion technique matches well with the $\bar{\varepsilon}_G$ obtained from GRT method using algebraic reconstruction technique. Fig. 5 shows the radial distribution of factional gas hold-up with V_G as a parameter. At lower V_G, the radial gas hold-up profile is flat representing the existence of homogeneous regime. With an increase in V_G, the radial gas hold-up profile becomes steeper and approaches a parabolic curve, representing the heterogeneous regime. The steeper gas hold-up profile leads to a higher time-averaged axial liquid recirculation velocity, which is responsible for pushing the gas bubble to the central region. The near wall gas hold-up also increases with an increase in V_G, however, the increase in the gas hold-up in the central region is more pronounced leading to higher $\Delta\varepsilon_G$, which is then responsible for the onset of heterogeneous regime and increased liquid circulation velocity.

The gas hold-up profile is relatively flatter until V_G = 0.055 m/s as can be seen from Fig. 5. This superficial velocity may be considered as the onset of transition regime which may extent up to $V_G \leq 0.084$ m/s. Here, it can be seen that the central region starts bulging in terms of larger bubbles and the near wall hold-up increases only slightly. Further increase in V_G increases the local fractional hold-up accordingly with a net increase of $\bar{\varepsilon}_G$. Thus, it is possible to find out or discern the regime transition from the nature of local gas hold-up distribution in a bubble column. An increase in free area from 0.42% to 1% increases

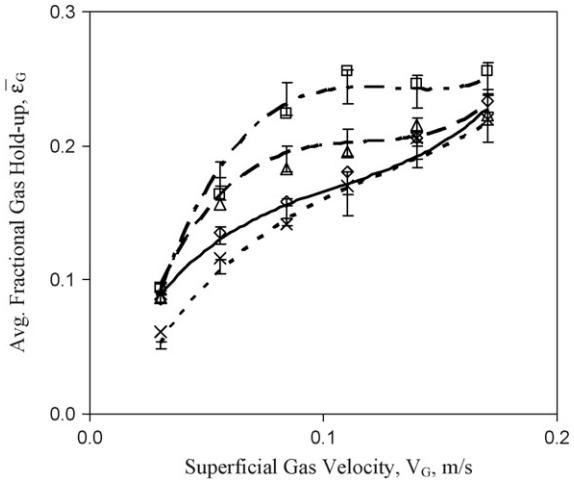

Fig. 4. Average fractional gas hold-up ($\bar{\varepsilon}_G$) vs. superficial gas velocity (V_G) for various sparger. Reconstructed values: ◊, S1; △, S2; □, S3; ×, S4; and measured values: —, S1; – – –, S2;– - –, S3; - - -, S4].

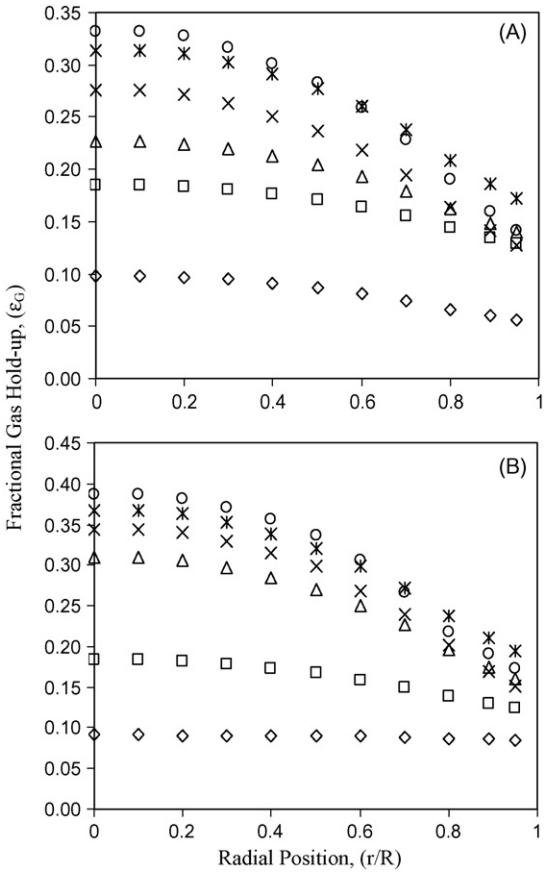

Fig. 5. Fractional gas hold-up profiles with superficial gas velocity as a parameter at $H/D = 0.785$ and hole dia. = 1 mm. (A) % free area = 0.42; (B) % free area = 1. ◊, 0.03 m/s; □, 0.055 m/s; △, 0.084 m/s; ×, 0.105 m/s; *, 0.14 m/s; ◯, 0.17 m/s.

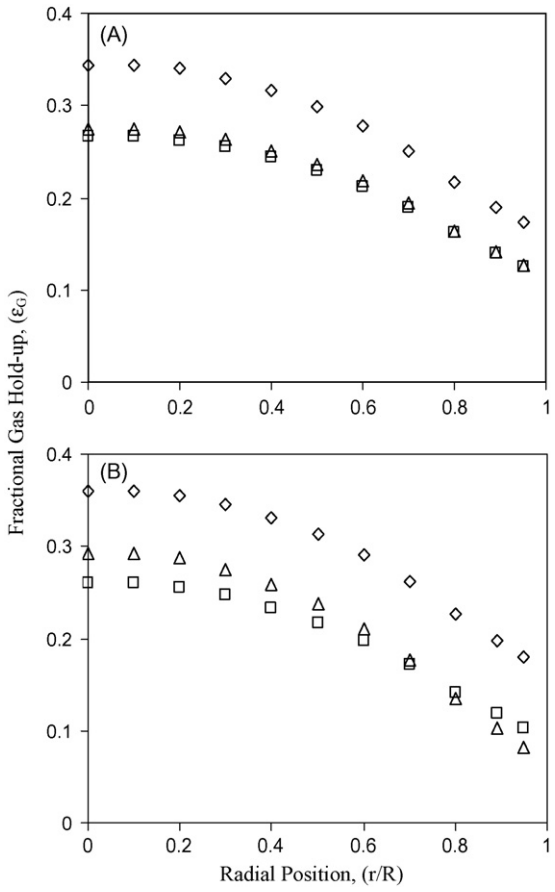

Fig. 6. Fractional gas hold-up profiles with % free area as a parameter at $V_G = 0.105$ m/s for perforated plate having hole dia. = 1 mm. (A) $H/D = 0.785$; (B) $H/D = 2.75$. □, 0.136%; △, 0.42%; ◊, 1%.

both local and average gas hold-up substantially in the region when $V_G \geq 0.084$ m/s, whereas, there is hardly any effect of the same at lower V_G as can be seen from Fig. 5A and B.

5.1.2. *Effect of % free area and hole diameter*

Fig. 6 shows the radial variation of fractional gas hold-up with % free area as a parameter. For the case of 0.001 m hole diameter, it can be seen that ε_G increases as a result of increase in free area from 0.136% to 1%. In case of lower free area plate, for example 0.136% and 0.42% and a given superficial gas velocity of 0.105 m/s, the gas issues in the form of a jet and the high velocity jets disappears in the continuous liquid medium at a distance away from the sparger plate. Further, the formation of larger coalesced bubble may also take place due to downstream interaction of jets. The lower ε_G in the case of these two spargers is mainly due to above reasons, where the gas issues as a jet at the speed of 80.77 and 25 m/s (hole velocity = V_G/free area) for 0.136% and 0.42% free area plates, respectively. It is therefore advisable to operate bubble column in such a way so that the gas does not issue in the form of jet, rather it issues as a bubble immediately from the sparger hole. The gas emerged from the 1% free area plate in the form of bubble rather than jet. At a hole velocity of 10 m/s corresponding to V_G of 0.105 m/s, it can be seen that the hold-up is substantially higher as compared to 0.136% and 0.42% free area. This observation was consistent for H_L/D of 0.785 and 2.75, as can be seen from Fig. 6A and B. The issue of jetting and its influence on bubble column hydrodynamics can be explained with the help of Weber number criteria given below [17]:

$$N_{We} = \frac{\rho_G d_o V_o^2}{\sigma_L} \leq 2 \tag{10}$$

In the jetting regime, the turbulence occurs at the orifice and the gas stream approaches the appearance of a continuous jet that breaks up 0.076–0.102 m above the orifice [17]. In the case of 1% free area sparger, the Weber number calculated using Eq. (10) for $V_G = 0.105$ m/s, is less than 2, an indication of no jetting. In the case of 0.136% and 0.42% free area spargers, N_{We} is obtained in excess of 10, which is much higher that the limits set by Eq. (10) and hence, the phenomenon of jetting causing adverse effect on bubble column hydrodynamics.

Fig. 7 shows the radial variation of ε_G with % free area as a parameter at $V_G = 0.17$ m/s. Here, it can be seen that the effect of % free area is minimal, although 1% free area gives higher ε_G at all radial locations. At a higher velocity of 0.17 m/s, ideal conditions are maintained for the churn turbulent regime. The near wall hold-up is found to be more at $H_L/D = 0.785$ than at

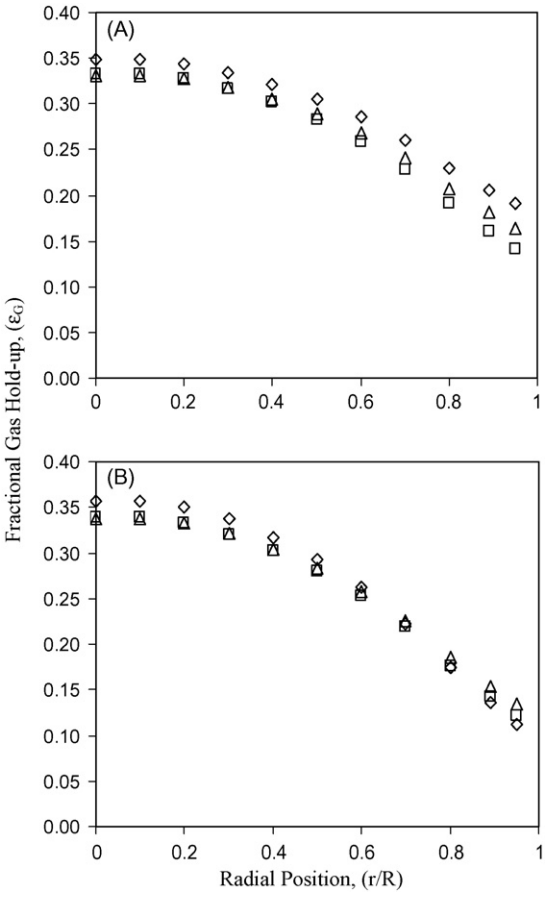

Fig. 7. Fractional gas hold-up profiles with % free area as a parameter at $V_G = 0.17$ m/s for perforated plate having hole dia. = 1 mm. (A) $H/D = 0.785$; (B) $H/D = 2.75$. □, 0.136%; △, 0.42%; ◇, 1%.

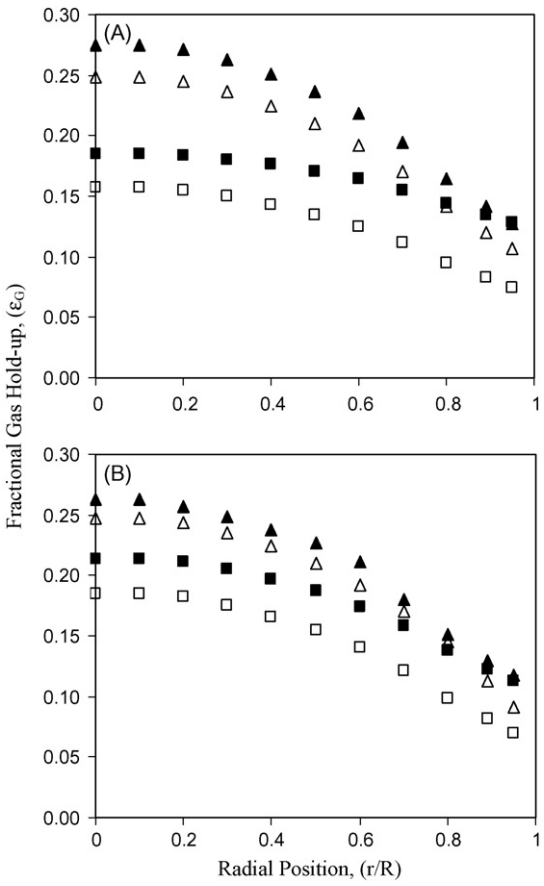

Fig. 8. Fractional gas hold-up profiles with plate hole size as a parameter for perforated plate having % free area = 0.42. (A) $H/D = 0.785$; (B) $H/D = 2.75$. At $V_G = 0.055$ m/s (■, 1 mm; □, 3 mm) and at $V_G = 0.105$ m/s (▲, 1 mm; △, 3 mm).

$H_L/D = 2.75$. These findings are in line with the reported results of Thorat et al. [16]. The average gas hold-up at $H_L/D = 2.75$ is lower than $\bar{\varepsilon}_G$ at $H_L/D = 0.785$ by as much as 30% as can be seen from Table 2. These finer aspects can only be analyzed with the help of GRT and the detailed hydrodynamic changes taking place over the entire cross-section can be visualized at several axial locations.

Fig. 8 shows the effect of hole diameter on the radial gas hold-up distribution of fractional gas hold-up. Hole diameter has a significant effect on ε_G as can be seen from Fig. 8A and B for two different H_L/D ratios. In both the cases, it can be seen that the lower hole diameter sparger plates are beneficial in maintaining higher $\bar{\varepsilon}_G$ across the entire bubble column. An increase in hole diameter from 0.001 to 0.003 m increases the primary bubble size thereby increasing the bubble rise velocity. These bubbles further coalesce to form bigger bubbles and they are pulled near the central region due to onset of liquid circulation [18]. Nevertheless, the strong effect of hole diameter for a given % free area can be considered equally important for maintaining a desired hydrodynamic configuration of bubble column. One of the major factor which influence the uniform gas distribution is its maintenance so as to avoid any clogging. The non-operating holes can have severe implications on the bubble column performance. The blockage of holes can be easily rectified with the help of GRT and the discussion to this effect is continued in the following section.

Table 2
Cross-sectional average gas hold-up in bubble column

Superficial gas velocity, V_G (m/s)	Sparger type	Cross-sectional average gas hold-up, $\bar{\varepsilon}_G$	
		$H_L/D = 0.785$	$H_L/D = 2.75$
0.105	S1	0.181	0.177
	S3	0.265	0.242
0.170	S1	0.231	0.228
	S3	0.266	0.253

5.1.3. Identification of gas distributor clogging

Fractional gas hold-up profile was obtained for various degree of clogging such as blockage to the extent of 75%, 50% and completely open. Fig. 9 depicts the two-dimensional gas hold-up distribution at two different axial locations of $H_L/D = 0.785$ and 2.75. At lower H_L/D ratio of 0.785, the effect of blockage can be seen as maximum as most of the portion is occupied by continuous phase liquid phase as can be seen by darker region in Fig. 9B. However, the effect of 75% blockage may not be obtained from Fig. 9C. Therefore, it is necessary to obtain the phase distribution near the

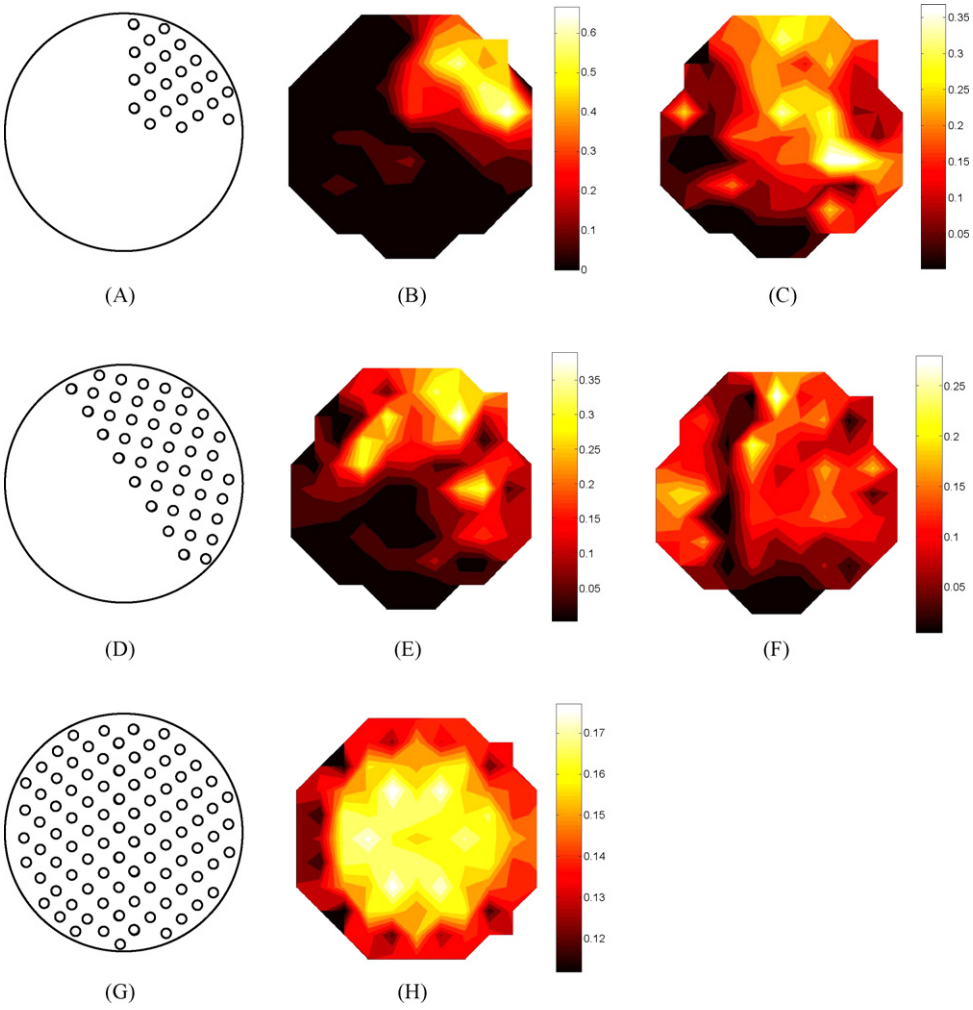

Fig. 9. Gas hold-up profile with sparger clogging as a parameter. For 75% clogging: (A) distributor plate; (B) at $H/D = 0.785$; (C) at $H/D = 2.75$. For 0% clogging: (D) distributor plate; (E) at $H/D = 0.785$; (F) at $H/D = 2.75$. For full open: (G) distributor plate; (H) at $H/D = 0.785$; (I) at $H/D = 2.75$.

region of clogging. It may be possible to correlate the average fractional gas hold-up as a function of V_G, but the exact nature of gas–liquid distribution near the sparger can only be unearthed by measuring the same under the prevailing operating condition. As H_L/D increases from 0.785 to 2.75, the lowering of $\bar{\varepsilon}_G$ or the uneven distribution of gas hold-up due to blockage of holes may take place due to several other factors such as influence of axial dispersion and indifferent turbulent eddies. Fig. 9E and F shows the gas hold-up profile distribution for 50% hole blockage and the region of higher and lower gas hold-up can be easily tracked in a similar as discussed above.

5.2. Case study—sectionalized bubble column

An industrial sectionalized bubble column of 0.3 m diameter having 10 sections divided equally over 8.5 m height was investigated by measuring radial gas hold-up profile. Gamma ray tomography was performed at four different sections. Sections 6–9 were selected due to their major influence on the overall hydrodynamic performance. In short, a chemical reaction takes place in this industrial unit whereby an acid and alcohol reacts to form an ester releasing hydrochloric gas as a co-product. The protocol demands for the reduction in gas phase backmixing and it is of prime importance to maintain the dissolved and free HCl gas to its lowest possible limit.

Fig. 10A–D shows the reconstructed images depicting the variation of gas hold-up at four different locations. The nature of gas hold-up profile is nearly similar to each other. The lower gas hold-up in the region away from the central core can be seen from these figures. This leads to an increase in $\Delta\varepsilon_G$ in the radial direction giving rise to extensive liquid circulation and therefore the increased gas phase backmixing. The present design of perforated plate having number of holes only in the central region of perforated plate is therefore undesirable from the point of view of maintaining minimal gas phase backmixing. The better design would be to have the same number of holes distributed uniformly over the entire cross-section of the perforated plate. If pressure drop is to be maintained same and if it is a fixed parameter, it may be desirable to have smaller holes and large number by keeping the same % free area of perforated plate.

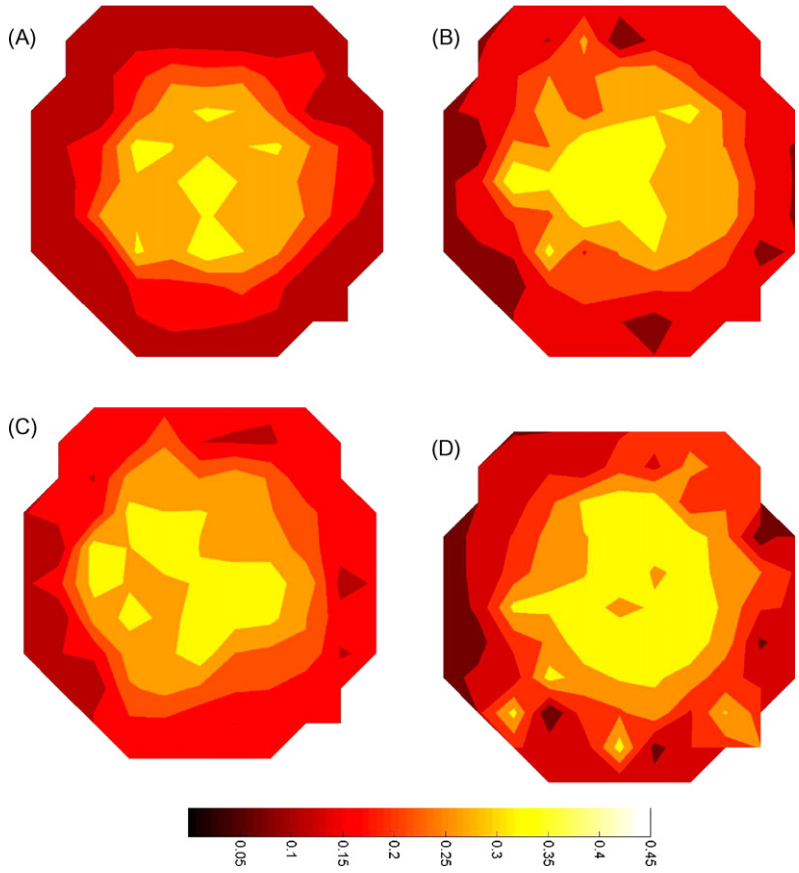

Fig. 10. Gas hold-up profile at four sections of sectionalizing bubble column. (A) 6th section; (B) 7th section; (C) 8th section; (D) 9th section.

Table 3 shows the average fractional gas hold-up values for four designated sections 6 to 9. It can be seen that $\bar{\varepsilon}_G$ increases from 21% to 25% as we move from sections 6 to 9, a clear indication of increased HCl concentration. The average fractional gas hold-up was analyzed with the help of Eq. (11) given by Doshi and Pandit [19]:

$$\bar{\varepsilon}_G = \left(0.7 + \left(0.055n - 0.43A_{RS} - 0.48\frac{D_{AS}}{D} - 0.055\frac{H_L}{D}\right)\right) \times V_G{}^{0.63} \quad (11)$$

The measured $\bar{\varepsilon}_G$ and the $\bar{\varepsilon}_G$ calculated using Eq. (11) match very well as can be seen from Fig. 11. As said earlier, $\bar{\varepsilon}_G$ has greater influence on the liquid phase residence time. An increase in $\bar{\varepsilon}_G$ will decrease the liquid phase residence time (τ_L) and may affect the conversion efficiency and the yield of the main product. The paramount importance of gas hold-up profile and τ_L, given by Eq. (12) can be understood precisely with the help of gamma ray tomography and algebraic reconstruction technique (ART):

$$\tau_L = \frac{V_D(1 - \bar{\varepsilon}_G)}{U_L} \quad (12)$$

The residence time of the liquid phase in the reactor is an important parameter to ensure the completion of reaction. Gas hold-up data was further utilized for the estimation of liquid phase residence time using Eq. (12) which was obtained as 1.9 h

Table 3
Cross-sectional average gas hold-up in sectionalizing bubble column

Section number	Average gas hold-up (%)
6	21.08
7	21.94
8	22.65
9	24.74

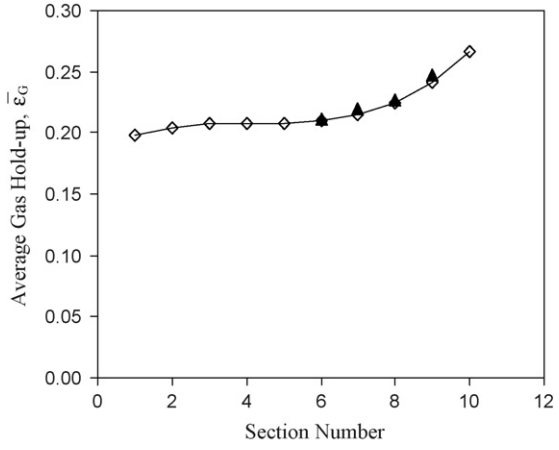

Fig. 11. Average gas hold-up values vs. section number: ◊, estimated using Eq. (11); ▲, estimated using GRT measurements.

for this system. This value was found to be in agreement with the desired reaction time for the completion of reaction.

6. Conclusion

The role of gamma ray tomography in understanding of bubble column in terms of local gas hold-up (ε_G) and average gas hold-up ($\bar{\varepsilon}_G$) was undertaken. The main emphasis was to obtain the effect of sparger design (including sparger clogging) on the gas hold-up distribution profile. The effect of superficial gas velocity on ε_G and $\bar{\varepsilon}_G$ for various sparger configurations was studied and the typical results are as follows:

- The use of GRT makes it easier to discern the regime transition. For example in 1% free area and 0.001 m hole diameter, the homogeneous regime prevails until $V_G = 0.055$ m/s. In the operating region of $0.055 < V_G \leq 0.084$ m/s, there exist the transition regime and when $V_G > 0.084$ m/s, heterogeneous regime sets in.
- The local gas hold-up as well as $\bar{\varepsilon}_G$ increases with an increase in % free area of the sparger for a given hole velocity. However, the effect of % free area is more in the homogeneous regime (Fig. 6) and substantial increase of $\bar{\varepsilon}_G$ can be made possible by choosing the correct free area of the sparger. In the heterogeneous regime of operation, there was minimal effect of % free area on $\bar{\varepsilon}_G$ as seen in Fig. 7.
- Weber number criteria can be used for discerning the transition taking place from bubbly flow to jetting flow:

$$N_{We} = \frac{\rho_G d_o {V_o}^2}{\sigma_L} \leq 2$$

- Maintaining Weber number of less than 2 is highly desirable from the point of view of avoiding jetting, particularly in low H_D/D bubble columns.
- An industrial sectionalizing bubble column of 8.5 m height and 0.3 m diameter was successful analyzed with the help of GRT. The hydrodynamic information obtained in terms of $\bar{\varepsilon}_G$ as a function of axial location was crucial in improving its performance. A change in sparger geometry could bring about substantial improvement in overall yield of the process.

References

[1] A. Kemoun, N. Rados, F. Li, M.H. Al-Dahhan, M.P. Duduković, P.L. Mills, T.M. Leib, J.J. Lerou, Gas holdup in a trayed cold-flow bubble column, Chem. Eng. Sci. 56 (3) (2001) 1197–1205.

[2] D. Toye, P. Marchot, M. Crine, A.-M. Pelsser, G. L'Homme, Local measurements of void fraction and liquid holdup in packed columns using X-ray computed tomography, Chem. Eng. Process. 37 (6) (1998) 511–520.

[3] M.B. Utomo, W. Warsito, T. Sakai, S. Uchida, Analysis of distributions of gas and TiO_2 particles in slurry bubble column using ultrasonic computed tomography, Chem. Eng. Sci. 56 (21/22) (2001) 6073–6079.

[4] A. Kemoun, S. Roy, M.H. Al-Dahhan, A.R. Cartolano, R. Dobson, J. Williams, Study of gas–liquid distribution in a pilot scale monolith reactor via industrial tomography scanner (ITS), in: Proceeding of 4th World Congress on Industrial Process Tomography, Aizu, Japan, 2005, pp. 220–225.

[5] U. Parasu Veera, A.W. Patwardhan, J.B. Joshi, Measurement of gas hold-up profiles in stirred tank reactors by gamma ray attenuation technique, Trans. Inst. Chem. Eng. 79 (A) (2001) 684–688.

[6] S. Banerjee, R.T. Lahey, Advances in Two-phase Flow Instrumentation in Advances in Nuclear Science and Technology, Plenum Press, New York, 1981.

[7] W. Snoek, A review of recent advances in multiphase flow measurements and methods, in: Experimental Heat Transfer, Fluid Mechanics and Thermodynamics, Elsevier, New York, 1988, pp. 59–71.

[8] A. Lubbert, B. Larson, Detailed investigations of the multiphase flow in airlift tower loop reactors, Chem. Eng. Sci. 45 (1990) 3047–3053.

[9] E.J. Morton, S.J.R. Simons, The physical basis of process tomography, in: D.M. Scott, R.A. Williams (Eds.), Frontiers in Industrial Process Tomography, Engineering Foundation, New York, 1995.

[10] R.A. Williams, M.S. Beck (Eds.), Process Tomography: Principles Techniques and Applications, Butterworth–Heinemann Ltd., 1995.

[11] J.B. Joshi, U. Parasu Veera, V. Prasad, D.V. Phanikumar, N.S. Deshpande, S.S. Thakre, B.N. Thorat, Gas hold-up structure in bubble column reactors, Proc. Indian Natl. Sci. Acad. (PINSA) 64 (4) (1998) 441–567.

[12] U. Parasu Veera, J.B. Joshi, Measurement of gas hold-up profiles by gamma ray tomography: effect of sparger design and height of dispersion in bubble columns, Trans. Inst. Chem. Eng. 77 (A) (1999) 303–317.

[13] U. Parasu Veera, J.B. Joshi, Measurement of gas hold-up profiles in bubble columns by gamma ray tomography: effect of liquid phase properties, Trans. Inst. Chem. Eng. 78 (A) (2000) 425–434.

[14] C. Kak, M. Slaney, Principles of Computerised Tomographic Imaging, IEEE Press, New York, 1988.

[15] A.K. Patel, A.W. Patwardhan, B.N. Thorat, Comparison of ML-EM algorithm and ART for reconstruction of gas hold-up profile in a bubble column, Chem. Eng. J. 130 (2–3) (2007) 135–145.

[16] B.N. Thorat, A.V. Shevade, K.N. Bhilegaonkar, A.V. Aglave, U. Parasu Veera, S.S. Thakre, A.B. Pandit, S.S. Sawant, J.B. Joshi, Effect of sparger design and height to diameter ratio on fractional gas hold-up in bubble columns, Trans. Inst. Chem. Eng. 76 (A) (1998) 832–833.

[17] J.R. Fair, D.E. Steinmeyer, W.R. Penney, B.B. Crocker, Gas absorption and gas–liquid system design, in: R.H. Perry, D.W. Green, J.O. Maloney (Eds.), Perry's Chemical Engineers' Handbook, 7th ed., McGraw-Hill, New York, 1997, pp. 14–71.

[18] J.B. Joshi, Axial mixing in multiphase contactors a unified correlation, Trans. Inst. Chem. Eng. 58 (3) (1980) 155.

[19] Y.K. Doshi, A.B. Pandit, Effect of internals and sparger design on mixing behavior in sectionalized bubble column, Chem. Eng. J. 112 (1–3) (2005) 117–129.